That value is very closed to $\delta_{opt.}$ For a constant gradient structure, $(\delta_o)_{B.I} = -g/2$. As an example $\Delta = (\delta_o)_{B.I} - \delta_{opt.}$ is tabulated below vs Δf for a SLAC section showing that the beam induction technique leads to a δ_o very close to the optimum even in the non-synchronous case.

Δf(kHz)	0	50	100	200
$\delta_{opt.}$(d°)	0	5,17	12,11	24,2
Δ	0	1,29	2,81	5,7

VI - EXTENTION OF ORSAY LINAC

Characteristics of the present machine:

— Maximum energy = 1,3 GeV obtained with 22 sections.

— Maximum straight ahead intensity: 80 mA peak.

— Beam pulse length = 1.5 μs.

— Total internal resistance = 2000 MΩ (2 MeV/mA).

— Energy spread: 50% of the straight ahead current within a 1% energy spread — up to 40 mA.

By adding:

— 16 sections and 16 klystrons of MW peak and 12 kW average we hope to get the following characteristics:

repetetion rate (p p s)	50	100	150
unloaded energy (GeV)	2,3	1.9	1,75
energy for a 80 mA beam (GeV)	2	1,7	1,45

— A positron couverter will be installed after the 8th section and will received a 100 MeV peak electron beam at 350 MeV.

REFERENCES

(1) G. A. Loew: Non-synchronous beam-loading in linear electron accelerators, ML Report No. 740 (Stanford, 1960).
(2) P. Brunet: Propriétés générales de la phase de l'onde hyperfréquence Accélérateur Linéaire, Onde Electrique, *435* (1963).
(3) J. M. Leiss and R. A. Schrack: Transient and beam-loading phenomena in linear electron accelerator, SLAC Doc 8 (Stanford, 1962).
(4) L. Burnod: Régime transitoire dans les accélérateurs linéaires, Laboratoire de l'Accélérateur Linéaire, Orsay, (thèse de 3ème cycle, 1961).
(5) R. B. Neal: Theory of the constant gradient linear electron accelerator, ML Report No. 513 (Stanford, 1958).
(6) R. B. Neal: Transient beam loading in linear electron accelerator, ML Report No. 388 (Stanford).

CHARACTERISTICS OF BEAM FROM THE ARGONNE ZGS INJECTOR LINAC*

R. Perry, P. V. Livdahl, E. A. Crosbie, G. E. Gallagher-Daggitt and W. W. Myers

Argonne National Laboratory, Argonne, Illinois (USA)

(Presented by R. Perry)

Since the Zero Gradient Synchrotron began operating two years ago, relatively little machine time has been available for making measurements of the characteristics of the injector system. Consequently, many details are yet to be studied.

LINAC PHASE ACCEPTANCE

Partial measurements have been made of the linac phase acceptance as a function of input ion energy and also as a function of the synchronous phase angle. In making these measurements, the buncher cavity is decoupled and the input beam is limited by two square aperture stops centered on the axis. The phase acceptance

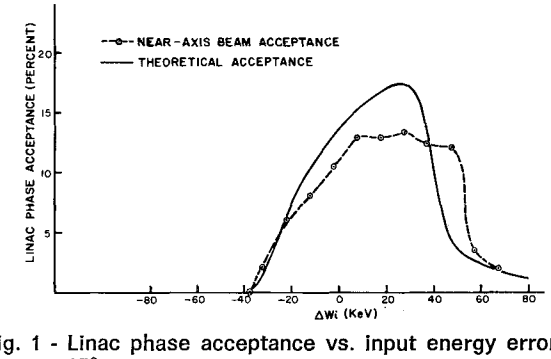

Fig. 1 - Linac phase acceptance vs. input energy error for $\psi_s = -15°$.

* Work performed under the auspices of the U. S. Atomic Energy Commission.

is taken to be that percentage of the input beam which is transmitted through the linac. Input and output beam were measured by ferrite-cored current transformers situated at the entrance and the exit of the linac. No correction is made for the possible presence of molecular (H_2^+) ions since we presently have no means of measuring the ion content of the beam at the linac entrance.

In order to determine the synchronous phase angle, it is necessary to establish the r.f. threshold for ion acceleration. This really involves extrapolation to zero beam acceleration from finite values. The accuracy of this determination and of the synchronous phase angle deduced therefrom, is limited by pulse-to-pulse jitter in the linac r.f. field level. Probable uncertainty in the threshold determination is about ± 0.5%.

Typical experimental results of the acceptance measurements are shown in Figs. 1, 2 and 3 where percentage transmission is shown as a function of input energy for synchronous phase angles - 15°, - 26° and - 30°, respectively.

For comparison with these experimental results, theoretical acceptance curves are also shown in the same figures. These have been calculated by

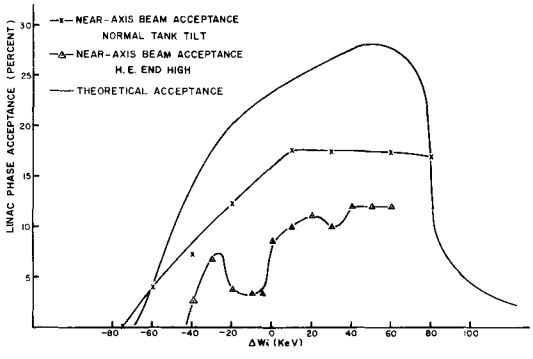

Fig. 2 - Linac phase acceptance vs. input energy error for $\psi_s = -26°$.

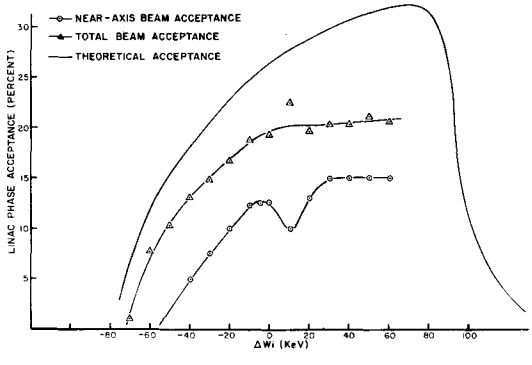

Fig. 3 - Linac phase acceptance vs. input energy error for $\psi_s = -30°$.

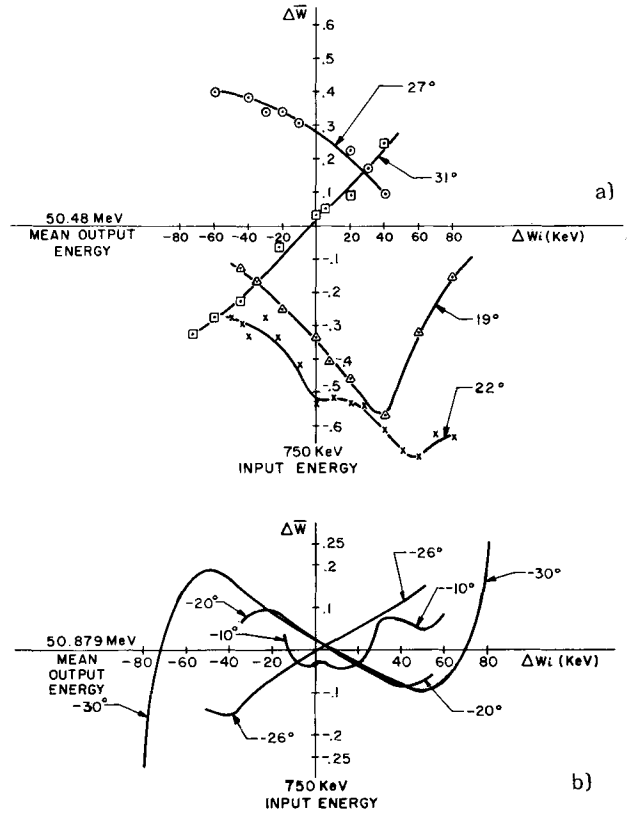

Fig. 4 - Mean energy of linac beam vs. input energy error with ψ_s as parameter: a) Experimental results. b) Computed for normal r.f. gradient.

Dr. D. E. Young of the MURA staff, using the PARMILLA computer program (1). The program has been corrected to include the variation of transit time factor with energy. The experimental results follow the theoretical trend for low input energy, but there is a tendency to flattening at higher input energies. In general, they fall below theoretical expectations. This can be explained for the most part by the presence of molecular ions in the injected beam.

The reason for this difference between experimental and theoretical results, particularly the dips or inverted peaks which some of the transmission curves exhibit, is not presently understood. However, we believe very strongly that the particular gradient distribution in the linac may have an important connection with this behavior. This view is supported by the fact that changing the gradient tilt by only a small amount has a remarkable effect on beam transmission. In the initial "flattening" of the linac cavity by perturbation methods, it was not conveniently feasible with the number of tuners available to set the relative gap voltages to the desired accuracy. Consequently, a compromise was arrived

at with some gaps being incorrect by as much as 10%, although most were within 5% of proper value.

We are presently contemplating a thorough recheck of the linac gradient distribution in an effort to arrive at a better understanding of its effect on transmission efficiency.

It has been noted that there is a greater transmission efficiency for the total beam than for near-axis beam injected through aperture stops (see Fig. 3). The measured emittance of the injected proton beam is well within the acceptance of the linac (2). However, inasmuch as the molecular beam is not focused by the matching triplets in the same manner as the proton beam, the molecular beam fraction will be different for the near-axis and for the off-axis portions of the beam. Consequently, the difference in apparent acceptance shown in Fig. 3 is believed to be primarily due to the difference in proton percentage in the input beam.

It is also interesting to note that in normal operation with the beam buncher the transmission efficiency is typically 50% to 60% of the total injected beam, which suggests that whatever is limiting the phase acceptance of the near-axis beam appears to have little influence upon the capture efficiency of the total bunched beam.

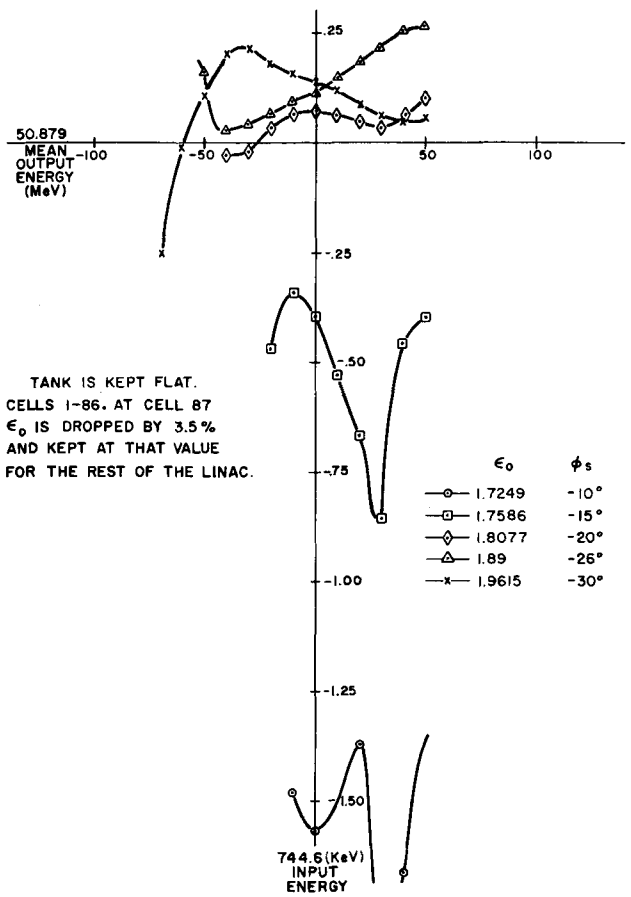

Fig. 5 - Computed mean linac beam energy with assumed 3.5% gradient step at middle of cavity vs. input energy error with ψ_s as parameter.

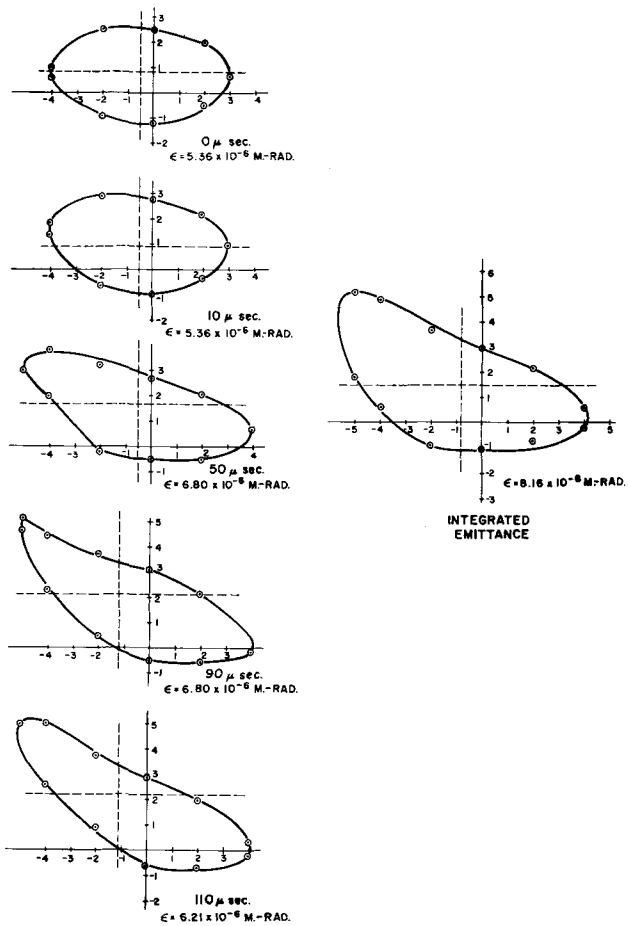

Fig. 6 - Time variation of linac beam emittance during 110 μsec pulse interval.

BEAM ENERGY MEASUREMENTS

The mean energy of the linac beam has been examined under the conditions of the previously described measurements using an energy monitor similar to that developed for the PLA at the Rutherford Laboratory (3). This device uses absorbers in the form of wedges one of which is variable, thus permitting sensitive adjustment of absorber thickness until half the particles are stopped in the absorber and half transmitted to a Faraday cup beyond. Null of a difference amplifier system gives sensitive indication of balance between the two currents. The absorber thickness is determined from the calibrated position readout of the adjustable wedge.

Variation of the mean energy with injection energy is shown in Fig. 4 (top) for several values of synchronous phase angle. These results show considerable vertical shift of mean energy with the linac r.f. level. However, computations carried out at MURA and shown in Fig. 4 (bottom) indicate that this vertical displacement should not be expected with a proper gradient distribution in the linac cavity. As a further check on this conclusion, a computer run was made for which a "flat" gradient was assumed in the first half of the linac with an abrupt drop of 3.5% for the last half of the cavity. This assumed distribution is a first attempt to simulate the mean distribution in the two halves of the linac as observed with calibrated loops. The results are shown in Fig. 5 which shows the type of separation found to exist in the actual measurements. Thus, we see further reason to question the gradient distribution.

TIME VARIATION OF BEAM POSITION AND EMITTANCE

When using segmented beam position detectors (4) to establish beam alignment between the linac and the ZGS, it is noted that a variation in lateral position of the beam center occurs during a beam pulse. This variation is repeatable from pulse to pulse and its magnitude and direction can be changed by varying the r.f. level. However, it is not possible to eliminate the effect by r.f. level adjustment.

Fig. 6 demonstrates that the beam steering effect is also accompanied by a variation of emittance of the linac beam during a pulse interval. Not only does the beam direction change by

Fig. 7 - Einzel lens section of accelerating tube with computed ion trajectories.

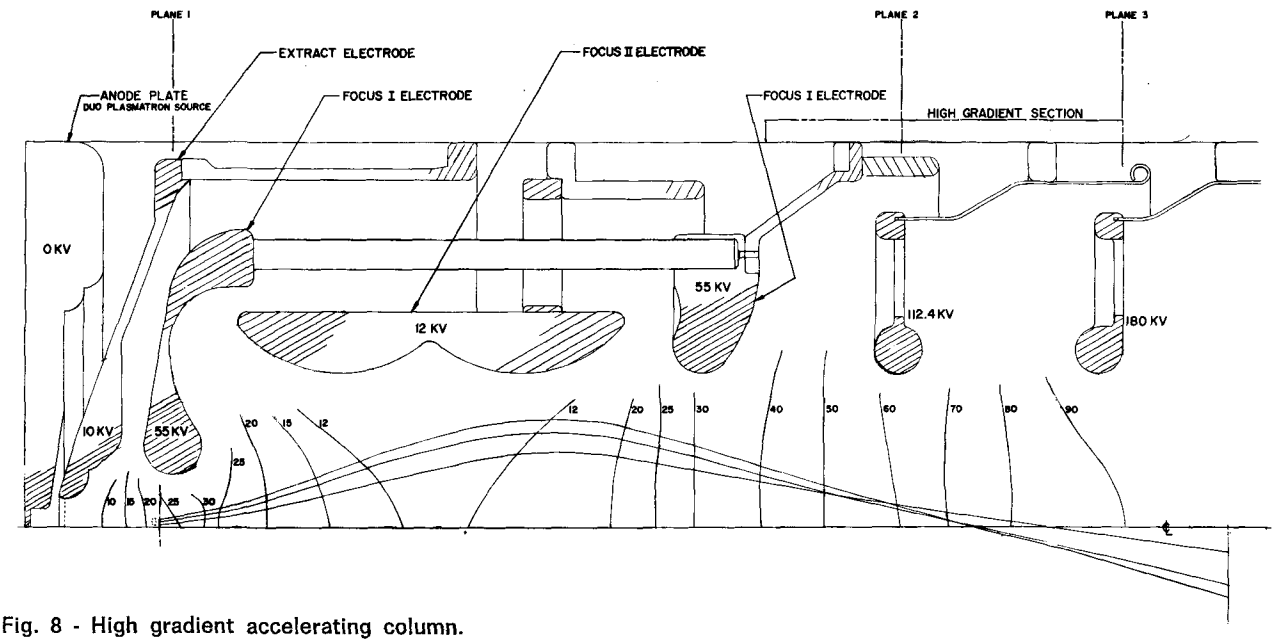

Fig. 8 - High gradient accelerating column.

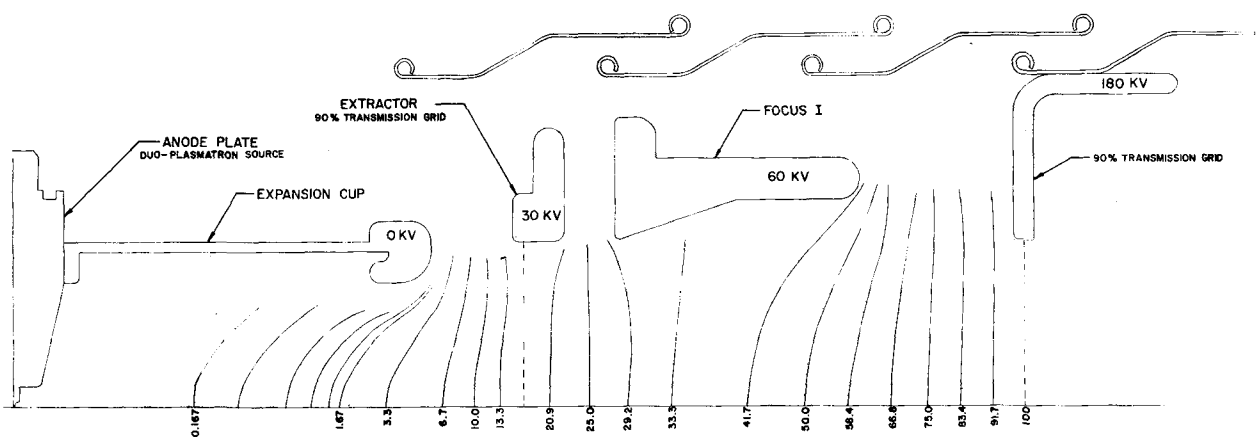

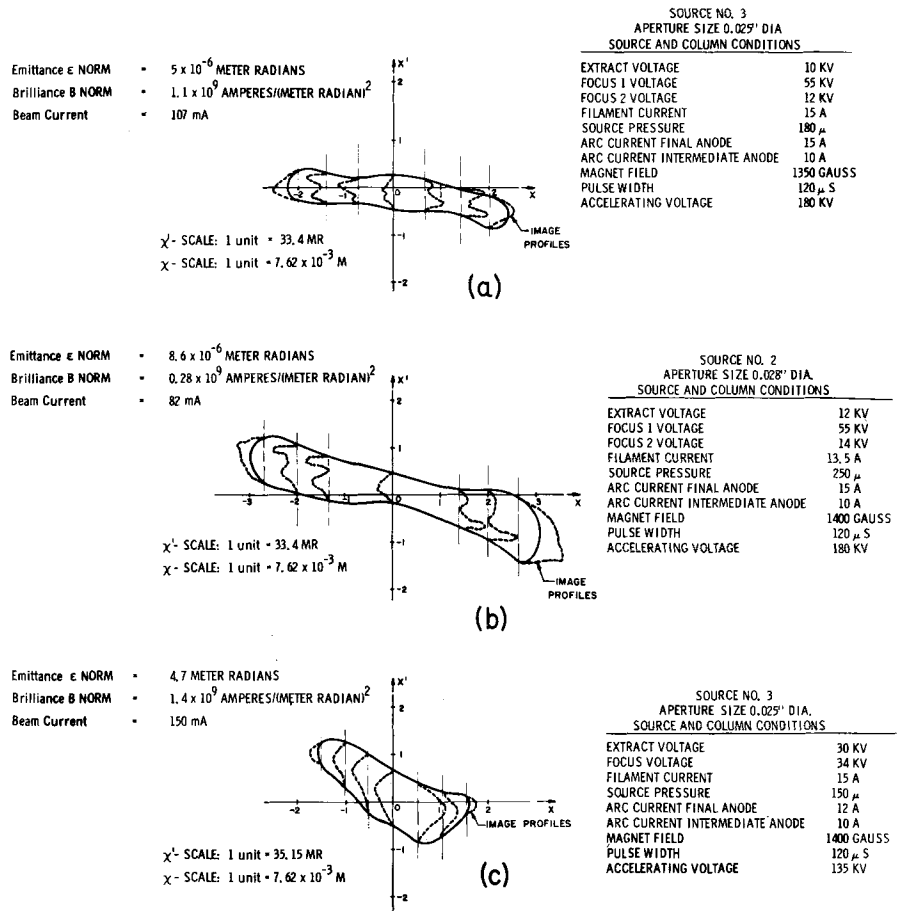

Fig. 9 - Emittance diagram.

a) Einzel lens geometry with duoplasmatron source No. 3.

b) Einzel lens geometry with duoplasmatron source No. 2.

c) High gradient column with modified duoplasmatron source.

about one milliradian during the 110 μsec beam pulse interval, but in addition the emittance area during this interval increases. The usual measurement of the beam emittance is the time integral of the instantaneous emittance and, as can be seen from the integrated emittance, Fig. 6 (right), it is of order of 30% larger than the maximum value of instantaneous emittance in this case.

Similar time analysis of the emittance of the 750 kV beam at the entrance to the linac shows that this phenomena does not exist at that point. It is therefore believed to be caused by the r.f. field in the linac cavity. It is plausible that this behaviour also may be a consequence of improper gradient distribution in the linac cavity.

COLUMN AND SOURCE STUDIES

Two accelerating column and source arrangements are being investigated at ANL.

a) An Einzel lens column which is an exact replica of the focusing section of the 750 keV preinjector column, Fig. 7. The system comprises a duoplasmatron source with a very small expansion cup, an extract electrode, a three-electrode Einzel lens and two electrodes which constitute a short high gradient section. The total accelerating voltage applied across the section is 180 kV.

b) An experimental short column which is based on the scheme investigated by Solnyshkov et al. (5). This arrangement, Fig. 8, was used in conjunction with the same source modified to receive a large expansion cup.

The facilities available in these investigations are: a 500 kV Cockcroft-Walton type dc accelerator together with apparatus for determining beam quality, an electrolytic tank for studying the fields due to various electrode configurations, and a computer to calculate beam trajectories from the data obtained from the electrolytic tank.

The following definitions (6) are used in describing the beam properties:

a) Normalized emittance $\varepsilon_{norm} = (A\beta\gamma/\pi)$ m radians, where A is the area of the emittance diagram in m radians.

b) Normalized brightness $B_{norm} = I/\frac{\pi^2}{2}(\varepsilon_{norm})^2$ amperes/ (m radians)².

c) I is the beam current in amperes.

Areas are determined using extreme values of divergence, which are measured by observing the image of a 0.020-inch object slit by means of a 0.010-inch diameter tungsten wire collector situated at a distance of 8.5 inches from the object slit. The resolution of the system is about 4% of the average emittance obtained.

Beam current is measured by means of a deep Faraday cup to which both a dc field and a transverse magnetic field are applied to eliminate error in measurement due to secondary electrons.

Data was obtained on the dependence of beam properties as a function of variables associated with the source parameters, and of the Einzel lens and extraction electrode potentials. It was found that the initial settings chosen to give maximum beam current to the Faraday cup also resulted in the best quality beam. A typical emittance diagram obtained is shown in Fig. 9 a. These investigations were repeated using another source of the same type and the conclusion was the same. In the second case, however, the emittance areas, Fig. 9 b, are greater by a factor of 2 to 3. This result is attributed to the larger extraction aperture, 0.028 inches compared with 0.025 inches in diameter in the first mentioned source.

Computer studies of particle trajectories indicate a waise in the beam in the high gradient gaps, Fig. 7. This has been suspected for some time. A computed emittance diagram, Fig. 10, is the result of tracing a beam of finite emittance (1.7×10^{-6} m radians), rectangular boundary and uniform density in phase space through the Einzel lens column. Gross aberration effects are evident. Exact comparison of computed with observed emittance results is not possible at this stage; however, some growth of the initial area is evident.

An emittance diagram for the short column is shown in Fig. 9 c and the quality factors for the

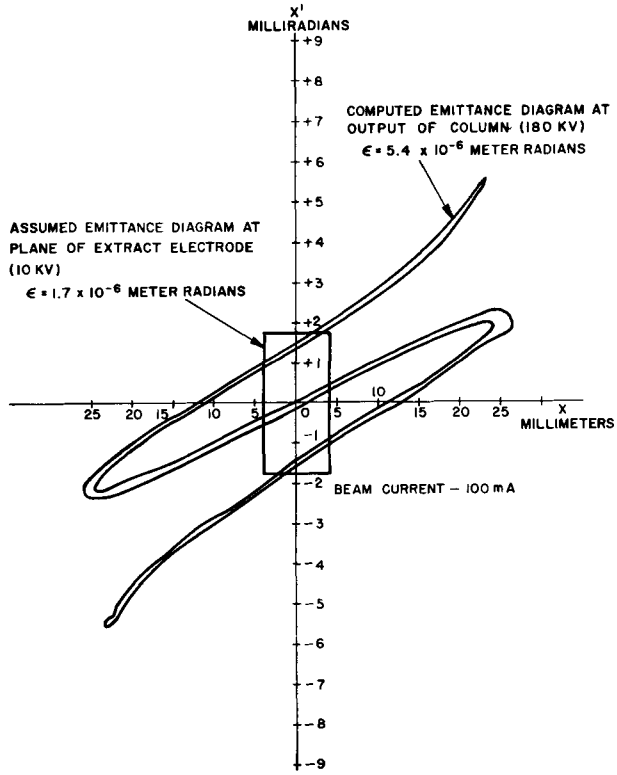

Fig. 10 - Computed emittance diagram from Einzel lens geometry shown in Fig. 7.

beam are based on a conservative estimate of the actual beam current whose measured value was 400 mA without dc bias applied to the Faraday cup. In this case, the beam profiles show no separation of beam from aberrations; whereas, in the Einzel lens geometry there is distinct separation into a core region surrounded by a ring, indicating that strong lens aberration exists in the Einzel lens system, but not in the high gradient geometry.

REFERENCES

(1) D. E. Young et al.: The Design of Proton Linear Accelerators for Energies Up to 200 MeV, MURA Report 713 (1965).
(2) D. Cohen: Review of Some Concepts Involved in ZGS Injection, Particle Accelerator Division Internal Report DC-3, (Argonne, 1962).
(3) R. C. Hannah and T. A. Hodges: PLA Progress Report, (Rutherford 1963) p. 111.
(4) E. A. Crosbie and P. V. Livdahl. Trans. on Nuclear Science, *NS-12*, No. 3, p. 799, (1965).
(5) Solynshkov et al :.Int. Conf. on High Energy Accelerators, Dubna, 1963, (Atomizdat, Moscow, 1964) p. 648.
(6) A. van Steenbergen: IEEE Trans. on Nuclear Science, *NS-12*, No. 3, p. 746, (1965).

DISCUSSION

MARTIN J. A.: You have had a second harmonic system under development. Could you comment on the results obtained?

PERRY: A short test of the 2nd harmonic system has been made but no improvement in beam transmission has observed. However, since the r.f. drive line to the 1st harmonic was at that time not in satisfactory condition the test of the effect of the 2nd harmonic cavity can hardly be considered valid. Further tests have not been possible because of the demands of the ZGS.